Experimental evidence for an original two-dimensional phase structure: An antiparallel semifluorinated monolayer at the air-water interface

A. El Abed,* M-C. Fauré, and E. Pouzet
Laboratoire Objets Complexes et Interfaces d'Intérêt Biologique (OCIIB), CNRS FRE 2303, Université René Descartes, 45 rue des Saints Pères 75006 Paris, France

O. Abillon
Laboratoire de Physique Statistique, CNRS UMR 8550 and Univerités Paris 6 and 7, Département de Physique de l'École Normale Supérieure, 24 rue Lhommond, 75005 Paris, France

(Received 12 November 2001; published 3 May 2002)

We show the spontaneous formation of an antiparallel monolayer of diblock semifluorinated *n*-alkane molecules spread at the air-water interface. We used simultaneous measurements of surface pressure and surface potential versus molecular area and performed grazing x-ray reflectivity experiments to characterize the studied monolayer, which is obtained at almost zero surface pressure and precedes the formation of a bilayer at higher surface pressure. Its thickness, equal to 2.7 nm, was found to be independent of the molecular area. This behavior may be explained by van der Waals and electrostatic interactions.

DOI: 10.1103/PhysRevE.65.051603 PACS number(s): 68.03.Cd, 61.10.Kw, 68.55.Jk

The presence of both a strong hydrophilic polar head and a long hydrophobic chain were believed, until the preliminary work of Gaines [1] in 1991 on semifluorinated *n*-alkane molecules, to be necessary to obtain stable Langmuir monolayers at the air-water interface [2]. Indeed, some semifluorinated alkanes [$F(CF2)_n(CH2)_mH$, denoted F_nH_m] can spread as Langmuir films although they carry no hydrophilic group. Therefore, the determination of their orientation at the air-water interface is a crucial point because both hydrogenated and fluorinated chains are known to be hydrophobic and nonmiscible, and also because of a large difference between the cross sections of fluorinated and hydrogenated blocks, respectively $A_F = 0.285$ nm^2 and $A_H = 0.185$ nm^2.

In the bulk state, F_nH_m compounds form lamellar phases, and more particularly smectic phases, whose structural characterization appears to be hard to achieve [3,4]. In two-dimensional (2D) systems, such as Langmuir monolayers, as well as the FH molecular packing, where fluorinated chains extend upward and hydrocarbon chains extend toward the water subphase, as suggested by Gaines [2] and Huang *et al.* [5] in their studies on $F_{12}H_{18}$ Langmuir monolayers, molecular dynamics simulations, carried out by Kim and Shin [6] on $F_{12}H_{18}$ monolayers, support the existence of an antiparallel molecular packing which will be denoted in this study as the FH/HF model.

Recently, we have shown that F_8H_{18} molecules form a stable condensed phase at the air-water interface, which we labeled the FH_2F phase, over a molecular area of about 0.30 nm^2. The FH_2F phase consists of a bilayer, whose thickness was found to be about 3.3 nm and where molecules orient antiparallel with respect to each other [7]. In such a bilayer, molecules extend their fluorinated chains outward and aggregate their hydrocarbon chains inward. Therefore, one may speculate upon the existence of a primitive monolayer from which the FH_2F bilayer builds up. In this article, we give experimental evidence for the existence of such a monolayer in the 0.45 nm^2–0.7 nm^2 molecular area range, at nearly zero surface pressure. This goal was achieved using surface pressure versus molecular area isotherm diagrams, surface potential measurements, and x-ray reflectivity experiments.

The F_8H_{18} compound used in this study was synthesized and purified (>98%) by M. Sanière of the René Descartes University (CNRS, UMR 8601) according to a well-known procedure [8]. At ambient temperature, it exhibits a crystalline phase whose structure is under investigation. The length and volume of a fully extended F_8H_{18} molecule may be calculated using tabulated numerical values [9]: $l_F \simeq 1.20$ nm, $l_H \simeq 2.44$ nm, $V_F \simeq A_F \times l_F = 0.34$ nm^3, and $V_H \simeq A_H \times l_H = 0.45$ nm^3.

The surface pressure (π) and surface potential (ΔV) versus molecular area (A) isotherm diagrams were recorded simultaneously using a Langmuir trough purchased from Nima Technology Ltd. The surface potential sensor consists of a commercial Kelvin probe (with an area of ~ 0.2 cm^2) which is suspended above the film spread at the air-water interface. Surface pressure, surface potential, and molecular area values were measured with an accuracy of, respectively, 0.1 mN/m, 10 mV, and 5%.

Figure 1 shows π-A and ΔV-A isotherm diagrams obtained simultaneously on compressing the film of F_8H_{18} at the air-water interface. Whereas the π-A isotherm diagram indicates the existence of a unique phase at a molecular area of about 0.3 nm^2, the ΔV-A isotherm diagram shows the occurrence of a phase transition in the 0.45 nm^2–0.3 nm^2 molecular area range.

The surface potential ΔV of a monolayer may be calculated, at a given molecular area A, according to the modified Helmoltz formula [10]

$$\Delta V = \frac{\mu_z}{A \epsilon_0 \epsilon}, \tag{1}$$

*Author to whom correspondence should be addressed.

 ©2002 The American Physical Society

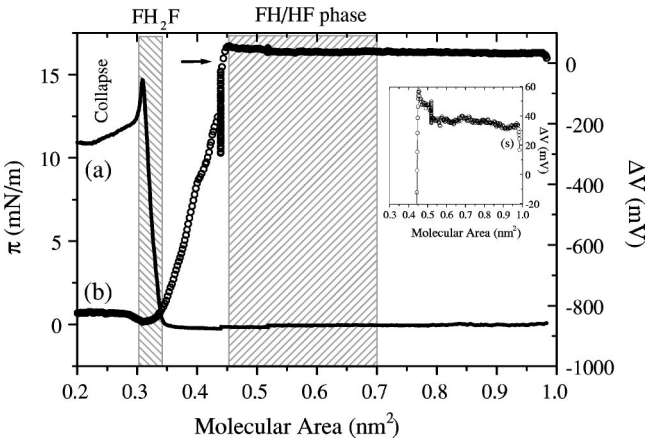

FIG. 1. Simultaneous surface pressure π (curve *a*) and surface potential ΔV (curve *b*) versus molecular area *A* isotherm diagrams obtained on compressing F_8H_{18} molecules at the air-water interface. The compression speed was about 3 cm^2/min and the Langmuir trough temperature was $T=23\,^{\circ}C$. Arrow indicates a stop for 10 min to allow for stabilization of ΔV.

where μ_z is the average vertical component of the molecular dipole moment $\vec{\mu}$, ϵ_0 is the permittivity of the void, and ϵ is the relative dielectric constant of the monolayer. ΔV is often assumed to result from the reorientation of hydrophobic chains under compression. Basically, the surface potential variation ΔV also results from a change, under compression, of the conformation of hydrophilic head groups and from the reorientation of water molecules underneath the monolayer. This is particularly true in the case of Langmuir monolayers of classical fatty acids where the hydrophilic -COOH head groups undergo strong anchoring at the water surface, but it is not valid in the case of F_nH_m molecules for which the hydrophilic head groups are missing. Consequently, the negative sign of the recorded surface potential in our experiment indicates that the vertical component $\langle \mu_z \rangle$ of the mean dipole moment of F_8H_{18} molecules is becoming oriented downward upon compression (i.e., from air toward the water subphase). More interesting is that the surface potential remains practically zero after the spreading of the film over molecular areas larger than 0.45 nm^2 (see Fig. 1). This means that the mean F_8H_{18} molecular dipole moment is equal to zero, $\langle \mu_z \rangle \sim 0$, for molecular areas larger than 0.45 nm^2. As we show in the following, the 0.45 nm^2–0.30 nm^2 region corresponds to a first order transition from a nonpolar monolayer to the previously characterized FH_2F bilayer [7]. The nonzero surface potential baseline is mainly inherent in the electric experimental setup: The baseline is shifted rapidly from 0 V to 40 mV approximately at the start of the film compression (see the inset of Fig. 1).

The linear decrease of surface potential ΔV vs molecular area *A* indicates the occurrence of a first order phase transition. Indeed, let us refer to the first phase and the second (FH_2F) phase as P_1 and P_2 phases. During the $P_1 \rightarrow P_2$ phase transition and according to the lever rule, the surface potential ΔV should vary linearly vs molecular area *A*, as shown:

$$\Delta V = \frac{A_1 \Delta V_2}{A_1 - A_2} + \frac{\Delta V_2}{A_2 - A_1} \times A = K_1 + K_2 \times A \qquad (2)$$

where $A_1 = 0.45$ nm^2 and $A_2 = 0.30$ nm^2 represent, respectively, molecular areas in the P_1 and the P_2 phases, as observed experimentally. Note that one has to move the compressing barrier very slowly (3 cm^2/min) and even has to stop it for several minutes at the beginning of the transition at about 0.43 nm^2 (see arrow on Fig. 1) in order to let ΔV stabilize to its equilibrium value. This pause is not necessary for other molecular areas.

The overall F_8H_{18} dipole moment $\vec{\mu}_{tot}$ may be subdivided into three components which are assigned to the terminal CF_3 group ($\vec{\mu}_F$), the CF_2-CH_2 junction ($\vec{\mu}_{FH}$), and the terminal CH_3 group ($\vec{\mu}_H$). It is oriented along the long axis of the molecule from the fluorinated chain toward the hydrogenated chain. Also, by analogy with the Demchack and Fort model [11], we consider the P_2 phase (FH_2F bilayer) as three superposed layers with three dielectric constants ϵ_3, ϵ_2, and ϵ_1 and three dipole moments $\mu = \mu_F + \mu_{FH}$, $\mu' = \mu_{CH_3} - \mu_{CH_3} \simeq 0$, and $-\mu = -\mu_{FH} - \mu_F$. Thus, the surface potential ΔV_2 of the FH_2F bilayer can be expressed as follows:

$$\Delta V_2 = \frac{2\mu}{A_2 \epsilon_0} \left(\frac{\cos\theta_3}{\epsilon_3} - \frac{\cos\theta_1}{\epsilon_1} \right) \qquad (3)$$

where θ_3 and θ_1 represent, respectively, tilt angles of $\vec{\mu}$ (which is associated with the terminal -CF_3 group and the -CF_2-CH_2- junction) in the lower and the upper layers. The $\vec{\mu}$ intensity has been calculated *ab initio* and was found to be about $\mu = 3.1$ D. Replacing μ, θ_3, and θ_1 by, respectively, 3.1 D, 28°, and 41° [7] in Eqs. (3) and (2), one finds $(0.75/\epsilon_1 - 0.88/\epsilon_3) \sim 0.55$. As far as we know, this is the first estimate of the problematic gradient of the dielectric constant across a Langmuir film, located at the interface of two media of very different dielectric constants such as water and air, respectively, 80 and 1. Thus, the jump of ΔV observed during the $P_1 \rightarrow P_2$ phase transition should be correlated with the location of the lower and the upper electric dipole moments, respectively, near the water and the air: The dielectric constant of a monolayer indeed depends on the surrounding phase [12,13].

The setup used for measurements of x-ray specular reflectivity of liquid surfaces was described elsewhere [14]. The characteristics of the x-ray beam are 0.154 nm for the wavelength λ; about 2×10^6 photons per second for the intensity; 8 mm for the horizontal width *w*; and 50 μm for the height *e*. As the x-ray reflectivity is a function of the vertical electron density profile, it gives information on the molecular packing. Experimental curves are fitted using classical optics with a one- or two-slab model [15]. The roughness σ of the interface induced by thermal fluctuations is also taken into account: It just adds a damping term $\exp(-q^2\sigma^2)$, *q* being the transfer wave vector [16]. Electron densities are derived from the area per molecule *A* and from the chemical composition and the thickness of the slab. As *A* is determined by the

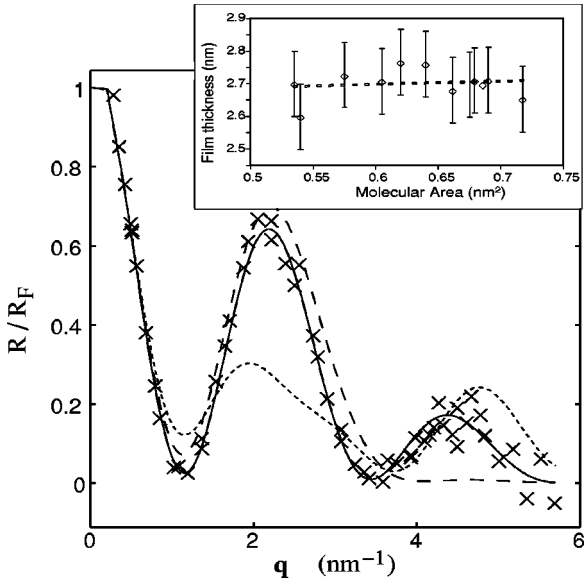

FIG. 2. Experimental reflectivity curves obtained from the F_8H_{18} film spread at the air-water interface over a molecular area $A=0.64$ nm^2. The full line corresponds to the best fit of the experimental points using the FH/HF model; the dashed line corresponds to the best fit of the experimental points using the FH model; the dotted line corresponds to the best fit of the experimental points using the HF model. Inset: Plot of the x-ray measured film thickness h_{meas} vs molecular area *A*.

Langmuir trough, the only free parameters of the model are the thickness of the slab and its roughness.

Figure 2 shows typical experimental x-ray reflectivity curves obtained for all molecular areas ranging between $A=0.70$ nm^2 and $A=0.45$ nm^2 (P_1 phase). For larger molecular areas, recording several successive x-ray reflectivity curves at fixed molecular area allows us to show that the film is not homogenous: For these molecular areas, the film consists of large domains that exhibit the reflectivity of the P_1 phase and domains that exhibit the reflectivity of an almost clean water surface, i.e., a gas phase. These observations allow for the estimation of the molecular area, $A\sim0.70$ nm^2, at which the P_1 phase becomes homogeneous, which cannot be deduced from π-*A* and ΔV-*A* isotherm diagrams.

The experimental curve in Fig. 2 shows typical Kiessig fringes damped by the surface roughness: The data are very well fitted by a one-slab model. The electronic density is thus constant along the vertical axis in the monolayer. Monolayer models with extra slabs (e.g., FH and HF models) do not fit the experimental curve if the thickness of the fluorinated slab is constrained to values below 1.2 nm, i.e., the length of a fully extended fluorinated chain (dashed lines in Fig. 2). Moreover, since FH and HF monolayers are polar, the surface potential ΔV would depart significantly from zero as the film is being compressed, and this not observed experimentally. For both these reasons the FH and HF models have to be rejected. On the contrary, an up-down FH/HF model, where statistically half of the molecules orient their fluorinated chains upward and the other half orient their fluorinated chains downward, can explain both the homogeneous

TABLE I. Fit parameter values of the experimental x-ray reflectivity curve, recorded at a molecular area of 0.64 nm^2, obtained using different packing models: FH, HF (with a limit on the fluorinated slab thickness of 1.2 nm), and FH/HF. h_1, h_2, and h represent, respectively, the thickness of the upper slab, lower slab, and overall film. The value found for the roughness σ of the film is typical at an air-water interface with a low surface pressure: For pure water, $\sigma=0.27$ nm.

Model	FH	HF	FH/HF
h_1 (nm)	1.20 (F)	2.61 (H)	
h_2 (nm)	1.25 (H)	1.20 (F)	
h (nm)	2.45	3.81	2.75
σ (nm)	0.45	0.24	0.30
χ^2	5.3	10	0.5

electronic density across the film and the nonpolarity of the monolayer. In order to get an estimate for the uncertainty on the ratio between the up and down molecules, one may note the existence of a small increase of ΔV, $+20$ mV (to be compared with the accuracy of 10 mV; see inset of Fig. 1) during the compression of the FH/HF phase. Applying Eq. 1 and assuming $\epsilon\sim1$ due to the low density of the monolayer in the FH/HF phase [10,13], such a difference would indicate that $\sim51\%$ of F_8H_{18} molecules point their electric dipole upward, i.e., their fluorinated chains downward.

The FH/HF model leads to a film thickness h_{meas} of about 2.7 nm. All fit parameter values are reported in Table I. It should be noted that this up-down organization must be fulfilled in an area smaller than the area of coherence A_C of the x-ray beam on the Langmuir trough. From the geometry of the experiment, a typical size of this area of coherence can be roughly estimated [15]: $A_C\sim(\lambda D/\pi)^2(ew)^{-1}\sim1000$ nm^2, where $D=0.4$ m is the distance between the x-ray source and the trough, and $ew=0.05\times8$ nm^2 is the geometry of the beam.

Let us now discuss the in-plane organization of the F_8H_{18} molecules according to the measured thickness value ($h_{meas}=2.7$ nm) of the FH/HF monolayer. If one assumes that F_8H_{18} molecules are at their maximum density, one may deduce a value of about $h_{calc}=(V_F+V_H)/A\simeq1.2$ nm for the thickness of the monolayer. This value is much smaller than the experimental value: The P_1 phase is far from a dense phase. On the contrary, if one assumes that the fluorinated chains are packed in nanodomains, oriented either up or down (see Fig. 3), and uses a simple geometrical analysis, one can calculate a monolayer thickness of about $h_{calc}=2.78$ nm. When packed, the thickness h_F of the fluorinated slab is equal to 1.20 nm, i.e., the total length of the rigid fluorinated chains; the 18 -CH_2- groups of each hydrogenated chain are then confined in a cylinder whose cross section is equal to $A_F\simeq0.28$ nm^2; the thickness h_H of the hydrogenated slab is then 1.58 nm. This calculated monolayer thickness, 2.78 nm, is in very good agreement with the measured value. The suggested nanodomain formation, which is also supported by the well-known tendancy of fluorinated chains to aggregate, leads to an overall surface fraction of void defects in the monolayer of about 50% at a

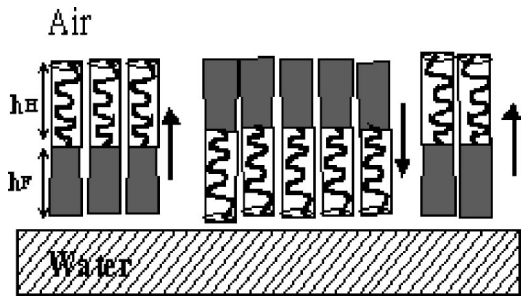

FIG. 3. Structure model for the FH/HF phase. Arrows show antiparallel orientation of mean nanodomain electric dipole moments.

molecular area $A=0.6\ \mathrm{nm}^2$. These voids are rather surprising but a plot of h_{meas} versus molecular area A (see the inset of Fig. 2) shows that the film thickness remains constant upon compression in the $A=0.7-0.5\ \mathrm{nm}^2$ range. This result suggests indeed the existence of voids in the monolayer which are progressively filled upon compression.

Let us finally discuss briefly some energetic aspects of the observed up and down structure. On one hand and on the basis of surface tension arguments, domains with their fluorinated chains oriented upward (domains up) would be favored compared to domains with their fluorinated chains downward (domains down). However, a rough calculation shows that the difference in energy between the two orientations is of the order of kT. On the other hand, the down orientation may also be favored because of hydrogen bonding and dipolar interaction between the termini C-F groups and the polar water molecules of the subphase. Thus, to better understand the physics of these original systems, it is necessary to perform a detailed theoretical study which, in addition to the above discussed effects, should take into account electrostatic interaction within and between the domains, van der Waals interactions, and line tension effects.

In conclusion, we have shown that the F_8H_{18} semifluorinated alkane forms a two-dimensional antiparallel monolayer (denoted FH/HF) at the air-water interface. The surface pressure of this monolayer is nearly zero and the area per molecule is between $0.7\ \mathrm{nm}^2$ and $0.45\ \mathrm{nm}^2$. Half of the F_8H_{18} molecules are oriented with their fluorinated chains downward, i.e., in contact with the water, and the other half with their fluorinated chains upward, i.e., in contact with the air. Experimental x-ray data are consistent with the organization of F_8H_{18} molecules in dense nanodomains and surface potential variation gives an estimate for the gradient of the dielectric constant across the monoalyer spread at the air-water interface.

[1] G.L. Gaines, Jr., Langmuir **7**, 3054 (1991).
[2] G. Gaines, Jr., *Insoluble Monolayers at Liquid-Gas Interfaces* (Interscience, New York, 1966).
[3] T.P. Russel, J.F. Rabolt, R.J. Twieg, and R.L. Siemens, Macromolecules **19**, 1135 (1986).
[4] P. Marczuck and P. Lang, Macromolecules **31**, 9013 (1998).
[5] Z. Huang, A.A. Acero, N. Lei, S. Rice, Z. Zhang, and M. Schlosmann, J. Chem. Soc., Faraday Trans. **92**, 545 (1996).
[6] N. Kim and S. Shin, J. Chem. Phys. **110**, 10 239 (1999).
[7] A. El Abed, E. Pouzet, M-C. Fauré, M. Sanière, and O. Abillon, Phys. Rev. E **62**, R5895 (2000).
[8] J.F. Rabolt, T.P. Russell, and R. Twieg, Macromolecules **17**, 2786 (1984).
[9] A. I. Kitaigorodsky, *Molecular Crystals and Molecules* (Academic Press, London, 1973).
[10] D.M. Taylor and G.F. Bayes, Phys. Rev. E **49**, 1439 (1994).
[11] R.J. Demchack and T.J. Fort, Jr., J. Colloid Interface Sci. **46**, 191 (1974).
[12] M. Iwamoto, Y. Mizutani, and A. Sugimura, Phys. Rev. B **54**, 8186 (1996).
[13] J.R. Macdonald and C.A. Barlow, Jr., J. Chem. Phys. **39**, 412 (1963).
[14] C. Postel and O. Abillon, Langmuir **14**, 5649 (1998).
[15] M. Born and E. Wolf, *Principles of Optics*, 6th ed. (Pergamon Press, New York, 1991), Chap. 1.6.
[16] J. Daillant and O. Belorgey, J. Chem. Phys. **97**, 5824 (1992).